2017 IEEE Conference on Control Technology and Applications (CCTA)
August 27-30, 2017. Kohala Coast, Hawai'i, USA

Piezoelectric Composite Subordinate Oscillator Arrays and Frequency Response Shaping for Passive Vibration Attenuation

Sai Tej Paruchuri[1], John Sterling[2], Andrew Kurdila[3] and Joseph Vignola[4]

***Abstract*— Subordinate Oscillator Arrays (SOAs) can be shown theoretically to provide vibration attenuation that is characterized by a frequency response function with a magnitude that is approximately flat over a finite bandwidth. However, the actual performance of SOA designs can suffer due to uncertainties in the structural parameters of the host and SOA. In this paper, we describe a piezoelectric composite SOA that can be used either actively or passively to account or correct for uncertainties in structural parameters that result from fabrication. This paper uses thermodynamic variational principles to derive the equations of motion for the active SOA formed using piezoelectric composites. We discuss techniques to optimize vibration attenuation for the SOA with fabrication errors using the piezoelectric appendages in the SOA.**

I. INTRODUCTION

Many researchers have studied the vibration absorption effects of attaching multiple substructures to a primary structure [1], [2], [6], [15]. These substructures have been referred to as Subordinate Oscillator Arrays, or SOAs. Reference [15], for example, has shown that careful prescription of distribution of the physical properties of the SOA can render flat the amplitude of a resonant peak in the frequency response function of the primary structure. The total mass of the SOA in this analysis can be relatively small when compared to that of the primary structure. In order to design the SOA, the structural properties of the primary structure and the SOA must be known precisely. In practice the SOA must be manufactured so that its properties match closely with the design specifications. The sensitivity of performance to errors in the properties of the primary structure and the SOA is also studied in [17]. It is shown that fabrication errors have a profound effect on the performance of the SOA.

For these reasons, the authors seek to model, design, fabricate, and test an SOA that has the potential to either optimize the structural properties, or to actively modify the structural properties, of the SOA to improve after-fabrication performance of the SOA. The fundamental design approach relies on the incorporation of piezoelectric appendages with appropriate shunt circuits into the SOA. The authors in [12] have derived the governing electromechanical equations of motion for such a piezoelectric composite SOA, and we have shown that changing the distribution of the shunt properties can achieve the desired flat frequency response for the SOA. We have likewise shown in [12] that the introduction of nonlinear switching strategies can effectively channel vibration energy into the shunt capacitor network of the SOA.

In this paper, the authors seek to extend the analysis in [15] to obtain analytic representations of the FRF from input excitation to primary vibration with the attached piezoelectric composite SOA. Such a representation will then facilitate the design of the composite piezoelectric SOA by providing analytic estimates of performance for the distribution of the structural properties of the SOA and distributions of the properties of the electrical properties of the attached shunt circuits.

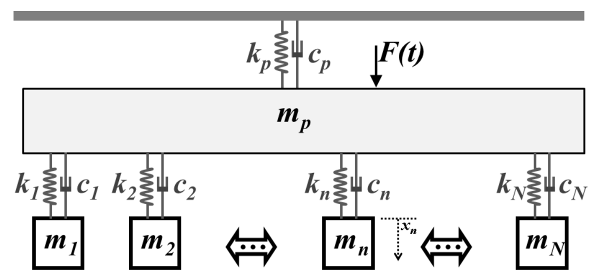

Fig. 1: A Host Structure with a Subordinate Oscillator Array (SOA): a Multi-Degree of Freedom System (MDOF) from [15], [17].

II. PIEZOELECTRIC SOA MODELING

A. Piezoelectric Composite Modeling using Variational Principle

Smart Material researchers have developed various formulation for modeling of linear as well as nonlinear piezoelectric structures. A review through early literature such as [14] would show that they were restricted to linear piezoelectric systems whereas emphasis on nonlinear piezoelectric systems modeling has been given in recent literature such as [18], [19]. The general approach used in all these studies involve a modified Hamilton's principle which is based on electric enthalpy density $\mathcal{H}$. A different approach for modeling of electromechanical systems is shown in [5]. It is shown that finite dimensional as well as infinite dimensional electromechanical systems can be modeled using charge or

[1]Sai Tej Paruchuri is a graduate student with the Department of Mechanical Engineering, Virginia Tech, saitejp@vt.edu
[2]John Sterling is a graduate student with the Department of Mechanical Engineering, Catholic University of America, jsterling@gmail.com
[3]Andrew Kurdila is a professor in the Mechanical Engineering Department,Virginia Tech, kurdila@vt.edu
[4]Joseph Vignola is a professor in the Department of Mechanical Engineering, Catholic University of America, vignoal@cua.edu

voltage variational methods. The approaches shown in [5] results in the Lagrange's equations for finite dimensional electromechanical systems in terms of displacement and charge or displacement and voltage as the generalized variable. The approaches summarized in [5] are also shown in [11]. But [11] further extends these approaches and introduces the extended Hamilton's principle to model linear piezoelectric systems. The approach can also be applied to piezoelectric systems coupled with shunt circuits with slight modifications. The governing equations of linear piezoelectric systems can be derived in terms of internal energy which is shown in chapter 5 of [8]. In the following subsection, we are going to introduce the variational principle that was used to model the the primary structure attached with a piezoelectric SOA.

B. $The \mathcal{V}_{\mathcal{H}}$-Variational Principle

The Hamilton's principle states that the actual trajectory followed by any mechanical system must satisfy the variational identity

$$\delta \int_{t_0}^{t_1} (T-\mathcal{V})dt + \int_{t_0}^{t_1} \delta W_{nc} dt = 0$$

for all possible variations in the configuration space. In the equation shown above, T is the total kinetic energy of the system, $\mathcal{V}$ is the total potential energy and δW_{nc} is the virtual work done by the non-conservative work done by the external forces acting on the system. The variational principle that is used to model linear piezoelectric systems is a modified form of the classical Hamilton's principle shown above. The variational principle to model a linear piezoelectric system will have the form

$$\delta \int_{t_0}^{t_1} (T-\mathcal{V}_{\mathcal{H}})dt + \int_{t_0}^{t_1} \delta W_{\mathcal{H},nc} dt = 0 \tag{1}$$

for all possible variations in the configuration space. The above equation has been expressed in terms of electric enthalpy density $\mathcal{H}$. In the above equation, T is the total kinetic energy of the system, $\mathcal{V}_{\mathcal{H}}$ is the potential that depends on the electric enthalpy density, displacements and flux linkages and $\delta W_{\mathcal{H},nc}$ is the virtual work done by the electromechanical loads on the system. This is the variational principle shown in Section 4.8 of [11]

C. Finite Dimensional Piezoelectric SOA Model

The overall configuration of the primary structure, the attached SOA, and the network of capacitive shunts attached to the linearly piezoelectric composite appendages is depicted in Figure 2. The variational formulation outlined in the previous subsection will now be used to derive the governing equations of primary structure with the attached composite piezoelectric SOA. The geometry of each substructure is shown in the Figure 3. The total kinetic energy for a SOA attached to a primary structure is written in the form

$$T = \frac{1}{2} m_p \dot{x}_p^2 + \sum_{i=1}^{N} \Bigg\{ \frac{1}{2} \int_0^{L_i} \rho_i A_i \left(\dot{x}_p + \frac{\partial w_i}{\partial t} \right)^2 dx_i + \frac{1}{2} m_i \left(\dot{x}_p + \frac{\partial w_i}{\partial t}(t, L_i) \right)^2 \Bigg\}.$$

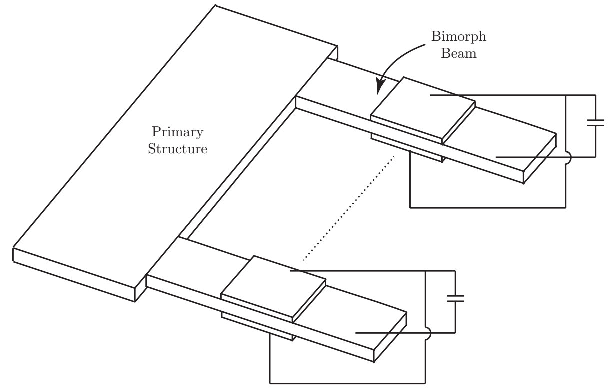

Fig. 2: The Host or Primary Structure, the Attached SOA, and the Capacitively Shunted Piezoelectric Composites.

where N is the number of sub-structures, x_p is the displacement of the primary structure, $w_i := w_i(t, x_i)$ is the displacement along each sub-structure i at the location $x_1(i)$, m_i is the tip mass attached to sub-structure i, L_i the length of the i^{th} sub-structure, ρ_i and A_i are the the mass density and cross-sectional area of the i^{th} sub-structure respectively. We use Galerkin methods to build approximations for the transverse displacement $w_i := w_i(t, x_i)$ of each appendage. We construct the approximation $w_i(t, x_i) = \sum_{k=1}^{n_i} \psi_{i,k}(x_i) w_{i,k}(t) = \boldsymbol{\Psi}_i^T(x_i)\boldsymbol{W}_i(t) = \boldsymbol{W}_i^T(t)\boldsymbol{\Psi}_i(x_i)$ for $i = 1, \ldots, n_i$, with the vectors $\boldsymbol{\Psi}_i$ and $\boldsymbol{W}_i$ defined as $\boldsymbol{\Psi}_i := \begin{Bmatrix} \Psi_{i,1} & \cdots & \Psi_{i,n_i} \end{Bmatrix}^T$ and $\boldsymbol{W}_i := \begin{Bmatrix} W_{i,1} & \cdots & W_{i,n_i} \end{Bmatrix}^T$. The total kinetic energy will have the form

$$T = \frac{1}{2} M_{pp} \dot{x}_p^2 + \sum_{i=1}^{N} \frac{1}{2} \bigg(2\boldsymbol{M}_{ip}^T \dot{\boldsymbol{W}}_i \dot{x}_p + \dot{\boldsymbol{W}}^T \boldsymbol{M}_{ii} \dot{\boldsymbol{W}}_i \bigg),$$

where $\boldsymbol{m}_{ii} := m_i \boldsymbol{\Psi}_i(L_i) \boldsymbol{\Psi}_i^T(L_i)$, $\boldsymbol{m}_{ip} := m_i \boldsymbol{\Psi}_i(L_i)$, $\mathcal{M}_i := \int_0^{L_i} \rho_i A_i dx_i$, $\boldsymbol{\mathcal{M}}_{ip} := \int_0^{L_i} \rho_i A_i \boldsymbol{\Psi}_i dx_i$, $\boldsymbol{\mathcal{M}}_{ii} := \int_0^{L_i} \rho_i A_i \boldsymbol{\Psi}_i \boldsymbol{\Psi}_i^T dx_i$, $M_{pp} := m_p + \sum_{i=1}^{N} M_i$, $M_i = \mathcal{M}_i + m_i$, $\boldsymbol{M}_{ii} = \boldsymbol{\mathcal{M}}_{ii} + \boldsymbol{m}_{ii}$, and $\boldsymbol{M}_{ip} = \boldsymbol{\mathcal{M}}_{ip} + \boldsymbol{m}_{ip}$. The expression for the electric enthalpy density for the

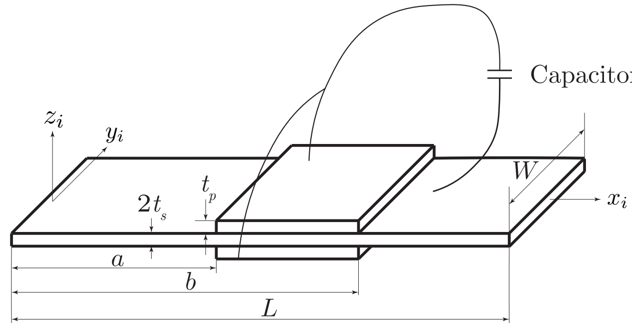

Fig. 3: Detailed Illustration of a Typical Piezoelectric Composite Appendage Connected to an Ideal Electrical Network

piezoelectric substructure has the form $\mathcal{H}_i := \frac{1}{2} C_i S_i^2 -$

$e_iS_iE_i - \frac{1}{2}\epsilon_i E_i^2$ where $E_i = E_i(x_i)$ is the electric field and S_i is the axial strain in the z_i direction. We use Bernoulli-Euler beam theory for simplifications of each sub-structure. Hence, the axial strain $S_1 = -z_i \frac{\partial^2 w_i}{\partial x_i^2}$. If $C_i = C_{11,i}^E$ is the stiffness coefficient, $e_i = e_{31,i}$ is the piezoelectric coefficient, $S_i = S_{11,i}$ is the axial strain in the x_i direction, $T_i = T_{11,i}$ is the axial stress in the x_i direction, $E_i = E_{3,i}$ is the electric field in the z_i direction, and $D_i = D_{3,i}$ is the electric displacement in the z_i direction, as per the linear piezoelectric constitutive laws, we have the relation

$$\begin{Bmatrix} T_i \\ D_i \end{Bmatrix} = \begin{bmatrix} C_i & -e_i \\ e_i & \epsilon_i \end{bmatrix} \begin{Bmatrix} S_i \\ E_i \end{Bmatrix}.$$

By the electrostatic approximation for linear piezoelectricity, the divergence of electric field is zero. We have the expression $E_i := E_{3,i} = -\frac{\partial \phi_i}{\partial z_i}$. Assuming that the potential across the piezoelectric strip in each sub-structure varies linearly, we obtain

$$E_i(x_i, y_i, z_i) = \begin{cases} -\frac{V_i}{t_{p,i}} & (x_i, y_i, z_i) \in \text{top patch}, \\ \frac{V_i}{t_{p,i}} & (x_i, y_i, z_i) \in \text{bottom patch}, \\ 0 & \text{otherwise}, \end{cases}$$

where V_i is the voltage across the piezoelectric strip. The electric enthalpy $\mathcal{V}_{H_i}$ of the substructure i can be expressed as $\mathcal{V}_{\mathcal{H}i} = \int_0^{L_i} A_i \mathcal{H}_i dx_i$. The electric enthalpy for the i^{th} substructure, after substituting the expressions for strain and electric field, has the form

$$\mathcal{V}_{\mathcal{H}i} = \int_0^{L_i} \left[\frac{1}{2} C_i I_i \left(\frac{\partial^2 w_i}{\partial x_i^2} \right)^2 - \frac{e_i \kappa_i}{t_{p,i}} \chi_{[a_i,b_i]} \frac{\partial^2 w_i}{\partial x_i^2} V_i \right] dx_i - \frac{1}{2} \frac{\epsilon_i 2A_{p,i}(b_i - a_i)}{t_{p,i}^2} V_i^2 - \frac{1}{2}\mathcal{C}_i V_i^2,$$

where $(C_iI_i)(x_i) := \int\int C_i z_i^2 dy_i dz_i$ and $\kappa_{T_i} := \int\int_{A_T} z_i dy_i dz_i$ for the top patch, $\kappa_{B_i} := \int\int_{A_B} z_i dy_i dz_i$ for the bottom patch, $\kappa_i := \kappa_{T,i} - \kappa_{B,i}$, and $\mathcal{C}_i$ is the capacitance of the capacitor attached to the piezoelectric strip.

We now substitute the same Galerkin approximation of the transverse displacement of the sub-structure i we substituted into the kinetic energy expression, $w_i(t, x_i) := \sum_{k=1}^{n_i} \psi_{i,k}(x_i) W_i(t) = \boldsymbol{\Psi}_i^T \boldsymbol{W}_i = \boldsymbol{W}_i^T \boldsymbol{\Psi}_i$. Now, we can express the electric enthalpy of the of the piezoelectric SOA attached to a primary structure as

$$\mathcal{V}_{\mathcal{H}} := \sum_{i=1}^{N} \left(\frac{1}{2} \boldsymbol{W}_i^T \boldsymbol{K}_{ii} \boldsymbol{W}_i - \boldsymbol{B}_i^T \boldsymbol{W}_i V_i - \frac{1}{2} D_i V_i^2 - \frac{1}{2} \mathcal{C}_{\rangle} V_i^2 \right) + \frac{1}{2} k_p x_p^2,$$

with the constants defined as $\boldsymbol{K}_{ii} := \int_0^{L_i} C_i I_i \boldsymbol{\Psi}_i'' \boldsymbol{\Psi}_i^{'',T} dx_i$, $\boldsymbol{B}_i := \int_0^{L_i} \frac{\kappa_i e_i}{t_{p,i}} \chi_{[a_i,b_i]} \boldsymbol{\Psi}_i'' dx_i$, and $D_i := \frac{\epsilon_i 2A_{p,i}(b_i - a_i)}{t_{p,i}^2}$.

We define new vectors and matrices in order to simplify the expressions of kinetic energy, electric enthalpy and non-conservative virtual work done. We have

$$\mathbb{W} := \begin{Bmatrix} \boldsymbol{W}_1 & \dots & \boldsymbol{W}_N \end{Bmatrix}^T, \quad \mathbb{V} = \dot{\mathbb{A}} := \begin{Bmatrix} V_1 & \dots & V_N \end{Bmatrix}^T,$$
$$\mathbb{A} := \begin{Bmatrix} \boldsymbol{\lambda}_1 & \dots & \boldsymbol{\lambda}_N \end{Bmatrix}^T, \quad \mathbb{M}_p := \begin{Bmatrix} \boldsymbol{M}_{1p} & \dots & \boldsymbol{M}_{Np} \end{Bmatrix}^T,$$

and define associated block matrices as

$$\mathbb{M} := \text{diag}(\boldsymbol{M}_1, \dots, \boldsymbol{M}_N), \quad \mathbb{B} := \text{diag}(\boldsymbol{B}_1, \dots, \boldsymbol{B}_N),$$
$$\mathbb{K} := \text{diag}(\boldsymbol{K}_{11}, \dots, \boldsymbol{K}_{NN}), \quad \mathbb{D} := \text{diag}(D_1, \dots, D_N),$$
$$\boldsymbol{\mathcal{C}} := \text{diag}(\mathcal{C}_1, \dots, \mathcal{C}_N).$$

The expressions for kinetic energy, electric enthalpy, and virtual work done can now be expressed as

$$T = \frac{1}{2}(\mathbb{M}_{pp}\dot{x}_p^2 + 2\dot{x}_p \mathbb{M}_p^T \dot{\mathbb{W}} + \dot{\mathbb{W}}^T \mathbb{M} \mathbb{W}),$$
$$\mathcal{V}_{\mathcal{H}} = \frac{1}{2}(\mathbb{W}^T \mathbb{K} \mathbb{W} - 2\mathbb{V}^T \mathbb{B}^T \mathbb{W} - \mathbb{V}^T \mathbb{D} \mathbb{V} - \mathbb{V}^T \boldsymbol{\mathcal{C}} \mathbb{V} + k_p x_p^2),$$
$$\delta W_{nc} = F\delta x_p - \delta x_p C_p \dot{x}_p - \delta \mathbb{W}^T \mathbb{C} \dot{\mathbb{W}}.$$

With the required expressions derived, we can now apply the extended Hamilton's principle to model our system. The kinetic energy, electric enthalpy and the virtual work done should satisfy equation 1. The variational statement stipulates that

$$\int_{t_0}^{t_1} \left\{ \mathbb{M}_{pp}\dot{x}_p \delta\dot{x}_p + \mathbb{M}_p^T \dot{\mathbb{W}} \delta\dot{x}_p + \dot{x}_p \mathbb{M}_p^T \delta\dot{\mathbb{W}} + \delta\dot{\mathbb{W}}^T \mathbb{M} \dot{\mathbb{W}} \right\} dt$$
$$- \int_{t_0}^{t_1} \left\{ \delta\mathbb{W}^T \mathbb{K} \mathbb{W} - \delta\mathbb{V}^T \mathbb{B}^T \mathbb{W} - \delta\mathbb{W}^T \mathbb{B} \mathbb{V} - \delta\mathbb{V}^T \mathbb{D} \mathbb{V} - \delta\mathbb{V}^T \boldsymbol{\mathcal{C}} \mathbb{V} + k_p x_p \delta x_p \right\} dt$$
$$+ \int_{t_0}^{t_1} \left\{ F\delta x_p - \delta\mathbb{W}^T \mathbb{C} \dot{\mathbb{W}} - \delta x_p C_p \dot{x}_p \right\} dt = 0$$

for all admissible variations. After performing standard procedures from variational calculus, we find that

$$\int_{t_0}^{t_1} \left\{ \delta x_p \left(-\mathbb{M}_{pp}\ddot{x}_p - \mathbb{M}_p \ddot{\mathbb{W}} - C_p \dot{x}_p - k_p x_p + F \right) + \delta\mathbb{W}^T \left(-\mathbb{M}_p \ddot{x}_p - \mathbb{M}\ddot{\mathbb{W}} - \mathbb{C}\dot{\mathbb{W}} - \mathbb{K}\mathbb{W} + \mathbb{B}\mathbb{V} \right) - \delta\mathbb{A}^T \left(\mathbb{B}^T \dot{\mathbb{W}} + \mathbb{D}\dot{\mathbb{V}} + \boldsymbol{\mathcal{C}}\dot{\mathbb{V}} \right) \right\} dt + \text{variational BCs} = 0\cdot$$

The above expression must hold for all admissible variations δx_p, $\delta\mathbb{W}$, and $\delta\mathbb{A}$ in the electromechanical configuration space. We conclude that the governing equations of the piezoelectric SOA attach to a primary structure are

$$\begin{bmatrix} \mathbb{M} & \mathbb{M}_p \\ \mathbb{M}_p^T & \mathbb{M}_{pp} \end{bmatrix} \begin{Bmatrix} \ddot{\mathbb{W}} \\ \ddot{x}_p \end{Bmatrix} + \begin{bmatrix} \mathbb{C} & \mathbf{0} \\ \mathbf{0}^T & C_p \end{bmatrix} \begin{Bmatrix} \dot{\mathbb{W}} \\ \dot{x}_p \end{Bmatrix} + \begin{bmatrix} \mathbb{K} & \mathbf{0} \\ \mathbf{0}^T & k_p \end{bmatrix} \begin{Bmatrix} \mathbb{W} \\ x_p \end{Bmatrix} - \begin{bmatrix} \mathbb{B} \\ \mathbf{0} \end{bmatrix} \mathbb{V} = \begin{bmatrix} \mathbf{0} \\ F \end{bmatrix}, \quad (2)$$

and

$$\mathbb{B}^T \dot{\mathbb{W}} + \mathbb{D}\dot{\mathbb{V}} + \boldsymbol{\mathcal{C}}\dot{\mathbb{V}} = \mathbf{0}\cdot \quad (3)$$

III. FREQUENCY RESPONSE FUNCTION

In [15], Vignola et. al. showed that prescribing the distribution of the properties of the SOA can be used to tailor the response of the whole system. In this section, we will derive the transfer function and the frequency response function from the force applied to the primary structure to its motion.

Integrating Equation 3 with respect to time and rearranging it, we get

$$\mathbb{V} = = -(\mathbb{D} + \boldsymbol{\mathcal{C}})^{-1}\mathbb{B}\mathbb{W}. \tag{4}$$

Equation 4 governs the voltage across the capacitor attached to each substructure in the SOA as a function of the displacement of the SOA. Taking the Laplace transform and substituting the result in Equation 2, we have

$$\begin{bmatrix} \mathbb{M}s^2 + \mathbb{C}s + \hat{\mathbb{K}} & \mathbb{M}_p s^2 \\ \mathbb{M}_p^T s^2 & M_{pp}s^2 + C_p s + k_p \end{bmatrix} \begin{Bmatrix} \mathbb{W} \\ x_p \end{Bmatrix} = \begin{bmatrix} \mathbf{0} \\ f(s) \end{bmatrix}, \tag{5}$$

with $\hat{\mathbb{K}} := \mathbb{K} + \mathbb{B}(\mathbb{D} + \boldsymbol{\mathcal{C}})^{-1}\mathbb{B}$.

We next seek to obtain a form for the Equations governing the primary and SOA that resembles that in reference [15]. In order to remove the mass coupling terms in equation 5, we introduce a change of variables which is given by

$$\begin{Bmatrix} \mathbb{W} \\ x_p \end{Bmatrix} = \begin{bmatrix} I & -\boldsymbol{\alpha} \\ \mathbf{0}^T & 1 \end{bmatrix} \begin{Bmatrix} \mathbb{X}_s \\ x_p \end{Bmatrix}$$

with $\boldsymbol{\alpha} = \mathbb{M}^{-1}\mathbb{M}_p$. Physically, the change of variables can be understood as introducing a suitably weighted measure of total displacement $\mathbb{X}_s := \mathbb{W} + \boldsymbol{\alpha} x_p$. Substituting the change of variables into equation 5 and pre-multiplying by the transpose of the matrix that defines the change of variables, we get

$$\begin{bmatrix} \mathbb{M}s^2 + \mathbb{C}s + \hat{\mathbb{K}} & -(\mathbb{C}s + \hat{\mathbb{K}})\boldsymbol{\alpha} \\ -((\mathbb{C}s + \hat{\mathbb{K}})\boldsymbol{\alpha})^T & \hat{M}_{pp}s^2 + \hat{C}_p s + \hat{k}_p \end{bmatrix} \begin{Bmatrix} \mathbb{X}_s \\ x_p \end{Bmatrix} = \begin{bmatrix} \mathbf{0} \\ f_p(s) \end{bmatrix} \tag{6}$$

where $\hat{M}_{pp} = (M_{pp} - \boldsymbol{\alpha}^T\mathbb{M}_p)$, $\hat{C}_p = (C_p + \boldsymbol{\alpha}^T\mathbb{C}\boldsymbol{\alpha})$, $\hat{k}_p = (k_p + \boldsymbol{\alpha}^T\hat{\mathbb{K}}\boldsymbol{\alpha})$. By introducing the change of variables, we have removed the off-diagonal mass blocks $\mathbb{M}_p$ and $\mathbb{M}_p^T$ from the equations of motion. From Equation 6, we have

$$\mathbb{X}_s = (\mathbb{M}s^2 + \mathbb{C}s + \hat{\mathbb{K}})^{-1}(\mathbb{C}s + \hat{\mathbb{K}})\boldsymbol{\alpha} x_p, \tag{7}$$

$$-((\mathbb{C}s + \hat{\mathbb{K}})\boldsymbol{\alpha})^T\mathbb{X}_s + [\hat{M}_{pp}s^2 + \hat{C}_p s + \hat{k_p}]x_p = f_p(s). \tag{8}$$

Equation 7 represents the relation between the motion of the substructures to the motion of the primary structure. We can get the transfer function relating the force applied to the primary structure to the motion of the same by substituting Equation 7 into Equation 8.

$$\frac{x_p(s)}{f_p(s)} = \Bigg\{ M_{pp}s^2 + C_p s + k_p + \sum_{n=1}^{N} \Bigg[-\alpha_n M_{p,n} s^2 + \alpha_n^2 C_{nn} s + \alpha_n^2 \hat{K}_{nn} - \frac{(C_{nn}\alpha_n s + \hat{K}_{nn}\alpha_n)^2}{M_{nn}s^2 + C_{nn}s + \hat{K}_{nn}} \Bigg] \Bigg\}^{-1} \tag{9}$$

It is imperative that the matrices $\mathbb{M}$, $\mathbb{K}$, $\mathbb{C}$, $\mathbb{B}$ and $\mathbb{D}$ are diagonal in order that Equation 9 holds. This is possible only when we use modal or Fourier shape functions. Also, the transfer function shown in Equation 9 holds for a single mode approximation although the transfer function for multiple mode approximation looks very similar. The frequency response function is now obtained by substituting $s = i\omega$ into Equation 9,

$$\frac{x_p(i\omega)}{f_p(i\omega)} = \Bigg\{ -M_{pp}\omega^2 + iC_p\omega + k_p + \sum_{n=1}^{N} \Bigg[\alpha_n M_{p,n}\omega^2 + \alpha_n^2 \Bigg[iC_{nn}\omega + \hat{K}_{nn} - \frac{(iC_{nn}\omega + \hat{K}_{nn})^2}{-M_{nn}\omega^2 + iC_{nn}\omega + \hat{K}_{nn}} \Bigg] \Bigg] \Bigg\}^{-1}. \tag{10}$$

The non-dimensional frequency response function can be obtained by dividing Equation 10 by the stiffness of the primary structure. The non-dimensional frequency response function is

$$\frac{x_p k_p}{f_p} = \Bigg[1 - \Omega^2 + \frac{i\Omega}{Q_p} + \sum_{n=1}^{N} \hat{\alpha}_n \Bigg[\Omega^2 + \frac{-\Omega^2\left(1 + \frac{i\Omega}{\beta_n Q_n}\right)}{1 - (\frac{\Omega}{\beta})^2 + \frac{i\Omega}{\beta_n Q_n}} \Bigg] \Bigg]^{-1}, \tag{11}$$

where

$$\begin{aligned} \Omega &= \omega\sqrt{\frac{M_{pp}}{k_p}}, & \tilde{\alpha}_n &= \frac{M_{nn}}{M_{pp}}, \\ \beta_n &= \sqrt{\frac{\gamma_n}{\tilde{\alpha}_n}}, & \gamma_n &= \frac{\hat{K}_{nn}}{k_p}, \\ Q_n &= \frac{\sqrt{M_{nn}\hat{K}_{nn}}}{C_{nn}}, & \hat{\alpha}_n &= \alpha_n^2\tilde{\alpha}_n. \end{aligned} \tag{12}$$

The analysis above yields a frequency response function for the SOA with capacitive shunts in Equation 11 that looks similar to the one shown derived for lumped systems studied in [15]. In the equation of the frequency response function, the term β_n is the non-dimensional frequency of each substructure. It is the frequency each substructure has when it is not connected to the rest of the system. It is obvious that the term γ_n does not appear in the final equation of the frequency response function because the non-dimensional mass $\tilde{\alpha}_n$, non-dimensional stiffness γ_n and the non-dimensional frequency β_n are related and interdependent. Q_n and Q_p represent the quality factor is the n^{th} substructure and the primary structure respectively.

IV. SOA DESIGN METHODOLOGY

Now that we have the expression for the frequency response function of the primary with the attached SOA, we can alter its response to excitation by varying the structural parameters of the SOA. Tailoring the frequency response function can be achieved by altering the distribution of mass properties, the distribution of structural stiffness, the distribution of capacitance, or a combination of these properties. We choose a distribution for β_n that was used by Vignola et. al in [15]. This distribution is expressed as

$$\beta_n = \begin{cases} \frac{\Delta}{2}\left(\left(\frac{2(n-1)}{N-1}\right)^p - 1\right) + 1 & \text{for } n \leq \frac{N}{2}, \\ \frac{\Delta}{2}\left(1 - \left(\frac{2(N-n)}{N-1}\right)^p\right) + 1 & \text{for } n \geq \frac{(N+1)}{2}. \end{cases} \tag{13}$$

The distribution function expressed in Equation 13 will generate β_n values that are centered at 1. The β_n values are distributed around the non-dimensional center frequency (that is equal to one) to form a band. The width of this band is decided by Δ. The term p in the distribution function is the exponent that decides the shape of the curve that prescribes the values of β_n.

In order to design the SOA, we first design a substructure whose resonant frequency matches that of the primary structure. Then we choose the distribution for the non-dimensional frequency. The non-dimensional mass of each substructure can be calculated using the relation shown in equation 12. The tip mass of each substructure is subsequently calculated using the expression

$$m_i = \frac{-(\tilde{\alpha}_n m_p + \tilde{\alpha}_n \rho AL) + \rho A \int \psi(x)^2 dx}{\tilde{\alpha}_n - \psi(L)^2}. \tag{14}$$

Using the above design strategy, we get a piezoelectric array in which each substructure differs only in terms of the tip mass.

It will often be convenient if we can select a fixed tip mass and instead vary the capacitance for each substructure. This would constitute a new method for modifying easily the SOA performance *post fabrication*. In this case, we calculate the non-dimensional stiffness instead of the non-dimensional mass. Then the capacitance for the n^{th} substructure circuit is given as

$$\mathcal{C}_n = \frac{B_n^2}{\hat{\mathbb{K}}_n - \mathbb{K}_n} - D_n. \tag{15}$$

V. RESULTS

The design strategies that were introduced in the previous section were implemented and frequency response of the primary structure with a piezoelectric SOA was simulated. The simulation was performed when $C = 6.9e+10$ Pa, $\rho_m = 2.3e+3$ kg/m^3, $N = 55$ $L = 0.5$ m, $w = 0.025$ m, $t = 0.003$ m, $a = 0.25$ L, $b = 0.75$ L, $t_p = 0.0005$ m, $e_{31} = -10.4$ C/ m^2, $\epsilon = 13.3$ nF/m, $m_p = 2000$ kg, $K_{pp} = 2.5466e+06$ N/m, $\zeta_{primary} = 0.0001$, $\zeta_{SOA} = 0.001$, $\mathcal{C} = 0$ F. Note that in this case, we considered a piezoelectric SOA with no capacitive shunts attached to it. Using the β_n values generated from equation 13 when $p = 1$ and $\Delta = 0.09$, the non-dimensional mass distribution was calculated using equation 12. The tip mass of each substructure calculated using equation 14 is shown in figure 5. Figure 4 shows the magnitude of the frequency response function that relates the displacement of the primary structure to the force applied on it when it is attached to an SOA with tip masses shown in figure 5. In the second case,

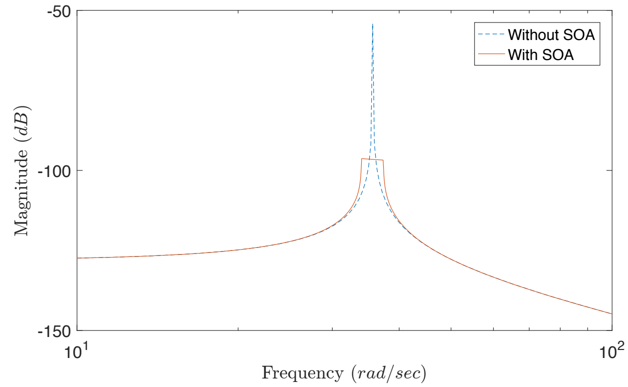

Fig. 4: Frequency Response Function from External Force Input to Displacement of the Primary Mass when the Tip Mass is Varied

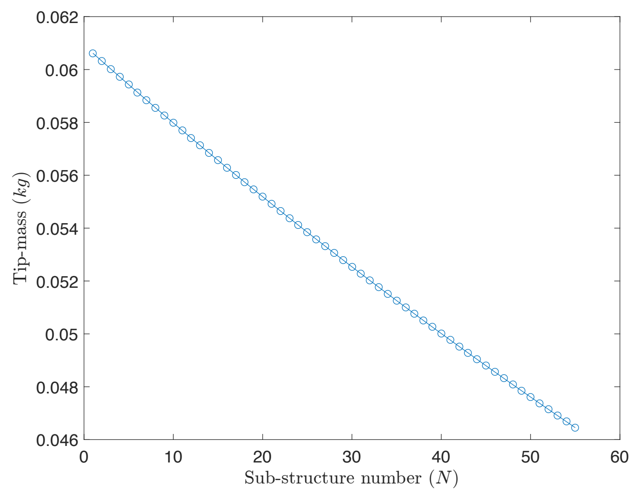

Fig. 5: Distribution of Tip Mass of Each Appendage that Results in Frequency Response shown in Figure 4

we considered a SOA with fixed tip masses and capacitive shunt circuits with varying capacitance attached to it. The simulation was performed with the same properties used in case 1 including the non-dimensional frequency distribution except $N = 55$, $K_{pp} = 1.2733e+06$ N/m, $t_p = 0.0015$ m and $m_{tip} = 0.00814$ kg. In order to reduce the effect of piezoelectric strips' capacitance, we attached a capacitor $\tilde{\mathcal{C}}_i = 1$ nF in series with each piezoelectric strip. The net capacitance $D_{i,net} = \frac{D_i \tilde{\mathcal{C}}_i}{D_i + \tilde{\mathcal{C}}_i}$ was used in the simulation of our system instead of D_i. The non-dimensional stiffness constant was calculated using the relation in equation 12. The capacitance of the capacitor attached to the substructures is calculated using the expression shown in equation 15. Figure 7 shows the distribution of the capacitance values calculated for this case. Figure 6 shows the frequency response function from the force applied to the primary structure to the displacement of the primary mass when the tip mass is kept constant and the capacitance values are varied as shown in figure 7.

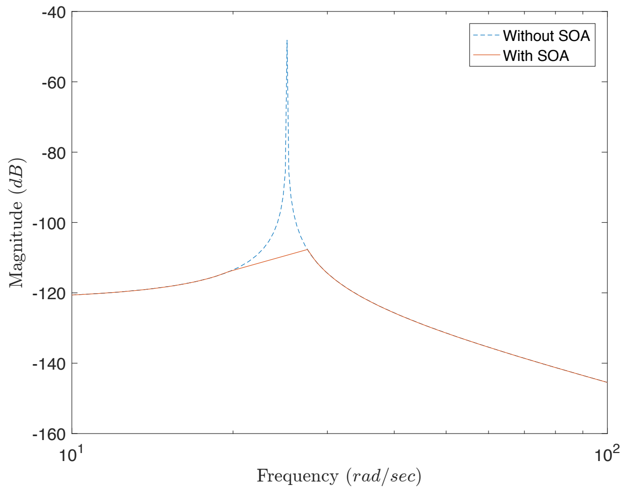

Fig. 6: Frequency Response Function from External Force Input to Displacement of the Primary Mass When the Network Capacitance is Varied

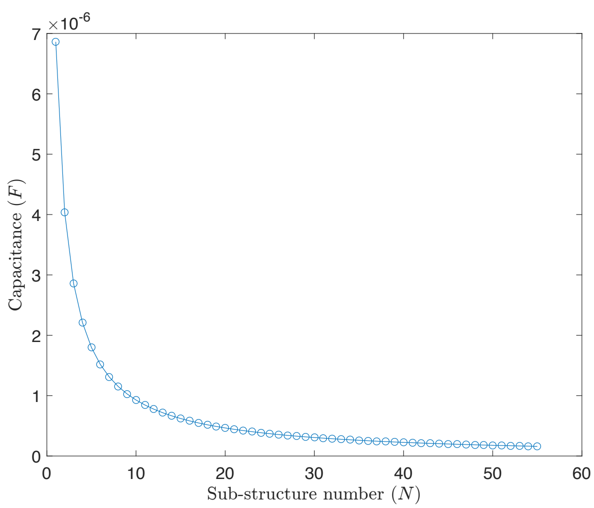

Fig. 7: Distribution of SOA Shunt Circuit Capacitance that Results in Frequency Response Shown in Figure 6

VI. CONCLUSIONS

This paper has introduced a strategy for tailoring the distributions of electromechanical properties of linear piezoelectric composite SOAs to achieve spectrally flat vibration attenuation near a resonant frequency of interest of the primary structure. The model of the the primary with the attached SOA is derived using the $\mathcal{V}_{\mathcal{H}}$-variational formulation for electromechanical systems that consist of linearly piezoelectric continua that are connected to ideal electrical networks. When a single mode approximation is used for representation of displacements in each appendage, the non-dimensional frequency response function from the external force applied to the primary structure to the displacement of the primary structure is obtained. With the introduction of a capacitive shunt network in the design, we show that it is possible to modify the distribution of capacitances in the shunt circuit to achieve spectrally flat vibration attenuation.

REFERENCES

[1] A. Akay, Z. Xu, A. Carcaterra, and I. Murat Koc, *Experiments on Vibration Absorption Using Energy Sinks*, *J. Acoust. Soc. Am.*, Volume 118, Number 5, pp. 3043-3049, 2005.

[2] A. Carcaterra, A. Akay, and C. Bernardini, *Trapping of Vibration Energy into a Set of Resonators: Theory and Applications to Aerospace Structures*, *Mechanical Systems and Signal Processing*, Volume 26, pp. 1-14, January, 2012.

[3] Christopher L. Davis, George A. Lesiutre, and Jeffrey J. Dosch, *Tunable Electrically Shunted Piezoceramic Vibration Absorber*, in *Smart Structures and Materials 1997*, pp. 51-59, *International Society for Optics and Photonics*, 1997.

[4] Woon Kyung Kim, *Design and Analysis of Switching Circuits for Energy Harvesting in Piezostructures*, PhD Dissertation, Virginia Tech, 2012.

[5] Dean C. Karnopp, Donald L. Margolis, and Ronald C. Rosenberg, *System Dynamics: Modeling, Simulation, and Control of Mechatronic Systems*, John Wiley & Sons, Inc., 2012.

[6] L. Kitis, B.P. Wang, and W.D. Pilkey, *Vibration Reduction Over a Frequency Range*, *Journal of Sound and Vibration*, Vol. 84, No. 4, pp. 559-569, August, 1983.

[7] Andrew J. Kurdila and Pablo Tarazaga, *Vibration of Linear Piezostructures*, John Wiley & Sons, Inc., in press, 2017.

[8] Donald J. Leo, *Engineering Analysis of Smart Material Systems*, John Wiley & Sons, Inc., 2007.

[9] G. Maidanik, *Induced Damping by a Nearly Continuous Distribution of Nearly Undamped Oscillators: Linear Analysis*, *Journal of Sound and Vibration*, Volume 240, pp. 717-731, 2001.

[10] Leonard Meirovitch, *Methods of Analytical Dynamics*, Macmillan, 1970.

[11] A. Preumont, *Mechatronics: Dynamics of Electromechanical and Piezoelectric Systems*, Springer, 2006.

[12] Sai Tej Paruchuri, Andrew Kurdila, John Sterling, Amelia Vignola, John Judge, Joe Vignola, and Teresa Ryan, *Thermodynamic Variational Formulations of Subordinate Oscillator Arrays (SOAs) with Linear Piezoelectrics*, *ASME 2017 International Design Engineering Technical Conferences & Computers and Information in Engineering Conference*, Cleveland, Ohio, August 6-9, 2017.

[13] M. Strasberg and D. Feit, *Vibration Damping of Large Structures Induced by Attached Small Resonant Structures*, *J. Acoust. Soc. Am.*, Volume 99, Number 1, pp. 335-344, 1996.

[14] Harry F. Tiersten, *Linear Piezoelectric Plate Vibrations*, Plenum Press, 1969.

[15] Joseph Vignola, John Judge, and Andrew Kurdila, *Shaping of a System's Frequency Response Using an Array of Subordinate Oscillators*, *Journal of the Acoustical Society of America*, Vol. 126, pp. 129-139, 2009.

[16] Joseph Vignola, Aldo Glean, John Judge, and Teresa Ryan, *Optimal Apparent Damping as a Function of the Bandwidth of an Array of Vibration Absorbers*, *The Journal of the Acoustical Society of America*, Volume 134, Number 2, pp. 1067-1070, August, 2013.

[17] Joseph Vignola, John Judge, John Sterling, Teresa Ryan, Andrew Kurdila, Sai Tej Paruchuri, and Aldo Glean, *On the Use of Shunted Piezo-Actuators for Mitigation of Distribution Errors in Resonator Arrays*, *Proceedings of the* 22^{nd} *International Congress on Acoustics*, Buenos Aires, September 5-9, 2016.

[18] Jiashi Yang, *An Introduction to the Theory of Piezoelectricity*, Springer, 2005.

[19] Yi-Yuan Yu, *Vibrations of Elastic Plates: Linear and Nonlinear Dynamical Modeling of Sandwiches, Laminated Composites, and Piezoelectric Layers*, Springer, 1996.